Compact Electron Beam or Light Ion Beam Fusion Reactor Cavity Design Using Non-Spherical Blast Waves

G.A. Moses and R. Spencer

April 1979

UWFDM-300

Nucl. Fusion Lett. 19, 1386 (1979).

FUSION TECHNOLOGY INSTITUTE

UNIVERSITY OF WISCONSIN

MADISON WISCONSIN

Compact Electron Beam or Light Ion Beam Fusion Reactor Cavity Design Using Non-Spherical Blast Waves

G.A. Moses and R. Spencer

Fusion Technology Institute
University of Wisconsin
1500 Engineering Drive
Madison, WI 53706

http://fti.neep.wisc.edu

April 1979

UWFDM-300

Nucl. Fusion Lett. 19, 1386 (1979).

Compact Electron Beam or Light Ion Beam Fusion Reactor Cavity Design Using Non-Spherical Blast Waves

Gregory A. Moses

Ross Spencer

Fusion Engineering Programment
Nuclear Engineering Department
University of Wisconsin

April 1979

UWFDM-300

Submitted as a Letter to Nuclear Fusion.
This work was supported by Sandia Laboratory, Albuquerque, N.M. under Contract #DSG/06-9329.

ABSTRACT

The application of inhomogeneous cavity gas densities and the non-spherical blast wave resulting from an explosion in this gas offers the potential to reduce the distance between the final diode and the target in a relativistic electron beam (REB) or light ion beam (LIB) fusion reactor. It can also sharply reduce the overpressure experienced by the diode after the target explosion.

1. Introduction

The concept of inertial confinement fusion first reported by Nuckolls, et al. in 1972[1] has received considerable attention in the ensuing years. With the emergence of larger lasers and relativistic electron beams as fusion drivers, the date for energy breakeven is now placed in the early to mid-1980's. Such rapid progress in the target physics necessitates increased attention to the problems associated with inertial confinement fusion (ICF) reactor design.

In this letter, particular attention will be given to reactor cavity designs for relativistic electron beam (REB) or light ion beam (LIB) driven fusion.[2] It has been proposed[3] that the reactor cavity in a REB or LIB fusion reactor be filled with gas at a density of 10^{18}-$10^{19}cm^{-3}$. This gas serves a dual role. First, it provides a background electron density for the establishment of ionized channels through which the REB or LIB is propagated from the final diode to the target.[2-3] Such channels might be initiated by laser breakdown using a low power laser.[2-3] Secondly, the gas provides a protection mechanism for the first wall. An unprotected first wall would not survive the surface heat load created by the X-rays and debris resulting from the target explosion at reasonable cavity size.[4] In the present approach, the X-rays and debris are absorbed in the gas. The debris is stopped in a small volume surrounding the target and a fireball is created which generates a strong spherical shock that propagates out to the wall. The minimum first wall radius and thickness are determined by stress levels generated by the overpressure created by this strong shock. In addition, the final diode must be protected from this overpressure and this places a limit on the distance between the diode and the target. This distance has been estimated to be about 4-5 meters for a target yield of 100 MJ.[3] Radiation damage to the first wall and diode may not place such a limit on cavity size. Hence, there is considerable interest in reducing the acceptable distance between the diode and the target so that the smallest possible reactor volume and hence the highest power density, can be achieved.

In this letter, we describe a variant of the gas filled cavity scheme that could greatly reduce the distance between the final diode and the target while still maintaining an acceptable overpressure at the diode and the first wall. This scheme relies on the dynamics of non-spherical blast waves that may be created by density and opacity gradients in the cavity buffer gas.

2. Non-Spherical Blast Waves

A point explosion in a homogeneous medium can often be described by strong shock theory.[5] In this case the pressure behind the spherical shock is given by

$$P_1 = \frac{3}{2\pi} \frac{\gamma^2-1}{3\gamma-1} \frac{E}{R^3} \tag{1}$$

where

$$R = \xi_o \left(\frac{E}{\rho_o}\right)^{1/5} t^{2/5} , \tag{2}$$

$$\xi_o \simeq \left[\frac{75}{16\pi} \frac{(\gamma-1)(\gamma+1)^2}{(3\gamma-1)}\right]^{1/5} , \tag{3}$$

γ is the ratio of specific heats, ρ_0 is the initial gas density, R is the distance from the center of the explosion to the shock front as a function of time, and E is the energy in the explosion. Kompaneets has extended this analysis to inhomogeneous gases.(6) In particular, he has looked at axisymmetric geometry where the gas density varies exponentially along the z-axis,

$$\rho_o = \rho_{oo} e^{-Z/\Delta} \tag{4}$$

In this case, $P_1(R)$ will be different depending on the direction of R relative to the z-axis. The explosive force will be vented down the density gradient, Fig. 1, so that the over-pressure experienced in directions (a) and (b) in Fig. 1, for a given value of R, will be less than that experienced in the case of a spherical blast wave for the same value of R. The pressure behind the shock in the non-spherical case is given by

$$P_1^* \approx \frac{2(\gamma^2-1)}{3\gamma-1} \frac{E}{\Omega} \tag{5}$$

where Ω is the volume enclosed by the shock front. This result is only correct for the limit of strong shock theory otherwise the pressure behind the shock must be replaced by $P_1^* - P_0$. It can be seen that the pressure in the nonspherical case is inversely proportional to the volume enclosed by the shock front just as in the spherical strong shock theory. Hence the shock pressure is smaller simple because the volume, Ω, is larger than in the spherical case. This enclosed volume must be computed using a numerical integration of the expression for Ω.(6) The details of this will not be included in this short letter.

3. Results

Using these expressions for the pressure behind the shock wave in the homogeneous and inhomogeneous cases the pressure as a function of distance from the point explosion can be compared for different directions relative to the density gradient. Fig. 2 is a plot of the pressure ratio, P_1^*/P_1, as a function of R/Δ in the directions denoted by (a) and (b) in Fig. 1. Note that the pressure ratio falls more rapidly in the (a) direction, up the density gradient, than it does in the (b) direction, perpendicular to the density gradient. Fig. 3 is a plot of $P_1(R)$ for the homogeneous case. From these two figures the absolute pressure in each case can be computed.

4. Discussion

These basic results can be used to great advantage in the design of REB or LIB fusion reactor cavities. As an example, if the scale height of the density gradient is $\Delta = 0.5$ m, then at a distance of 1.05 meters from a 30 MJ explosion (100 MJ total yield) the pressure perpendicular to the density gradient is 5 atm. This is to be compared to a value of 50 atm in the homogeneous case. Up the density gradient the pressure falls to zero at 1.05 meters. If a density gradient can be tolerated along the ionized channel direction, this analysis would imply that the overpressure in the direction of the channel can be further reduced. The use of inhomogeneous cavity gases will allow more freedom in the choice of the distance from the diode to the target. With this overpressure constraint now removed, this distance will likely be determined by neutron damage effects to the diode.

Clearly there are many questions that remain to be analyzed before a final conclusion can be drawn. A density gradient with the proper scale length must be established. Such a gradient might in fact be created by the use of two different layered gases (see Fig. 4). When the shock front reaches the interface between the gases the low opacity gas "vents" the energy from the fireball reducing the shock in the heavier gas. A variety of different "engineering solutions" to the density (or opacity) gradient need to be investigated. Solutions for the pressure as a function of R must be generated for density profiles other than an exponential. Although the analytical results predict that the pressure ratio P_1^*/P_1 goes to zero at finite radius this is clearly unphysical. In actuality, there is a transition from strong to weak shock theory. We note that in the homogeneous case,[3] strong shock theory begins to breakdown for a 25.8 MJ explosion in 100 Torr of N_2 at about a radius of 3-4 meters. At 3 meters strong shock theory predicts a pressure of 1.3 atm but the actual pressure is 2 atm. Alternatively, the pressure is 1.3 atm at 3.5 meters rather than 3 meters. Hence the predictions of strong shock theory are roughly valid for $P_1/P_0 \gtrsim 10$. If P_0 = 50-100 Torr, then analysis of cavities with overpressures of ~1 atm will be near the range of validity for this approximation. More exact results will likely require two-dimensional hydrodynamics calculations.

5. Conclusions

The application of an inhomogeneous cavity gas density and the non-spherical blast wave resulting from an explosion in this gas offers the potential to reduce the distance between the final diode and the target in a REB or LIB fusion reactor. It might also greatly reduce the overpressure experienced by the diode after the target explosion. Such a result addsto the potential of REB or LIB fusion as an attractive candidate for reactor applications.

Acknowledgement

This work was supported by Sandia Laboratory, Albuquerque, New Mexico.

References

1. J. Nuckolls, et al., Nature 239, 139 (1972).

2. G. Yonas, Sci. Am. 239, 50 (Nov. 1978).

3. D. Cook and M.A. Sweeney, "Design of Compact Particle-Beam-Driven Inertial-Confinement Fusion Reactors", Proc. of 3rd ANS Meeting on the Tech. of Controlled Nuclear Fusion, Santa Fe, NM, May 1978.

4. R. Conn, J. Nucl. Mats., 76/77, 103 (1978).

5. L. Sedov, Prikl. Mat. i Mekh. 10, 241 (1946) and G. Taylor, Proc. R. Soc. A 201, 159 (1950).

6. A.S. Kompaneets, Soviet Physics "Doklady" (English Trans.) 5, No. 1, 46 (1960). Also see Zel'dovich and Raizer, Physics of Shock Waves and High-Temperature Hydrodynamic Phenomena, Vol. II, Academic Press (New York, 1967), p. 849.

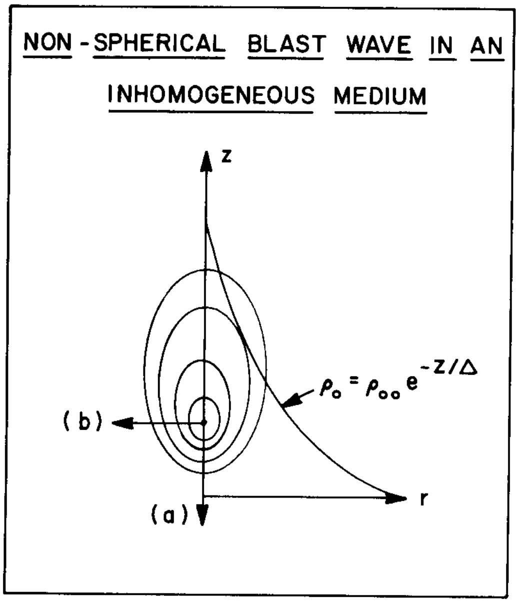

Fig. 1

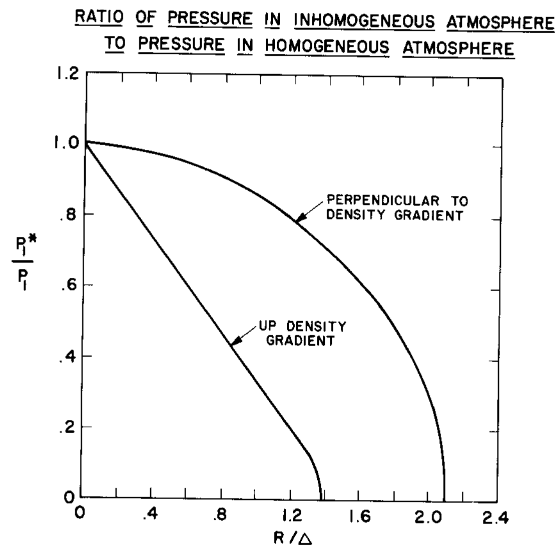

Fig. 2

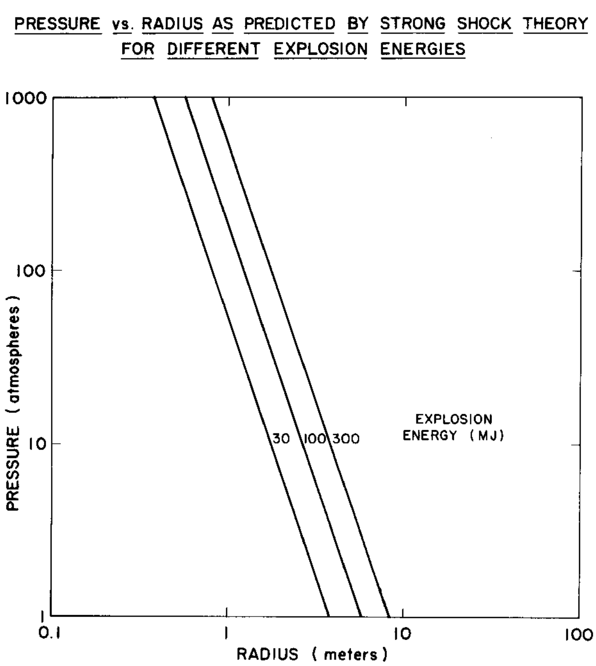

Fig. 3

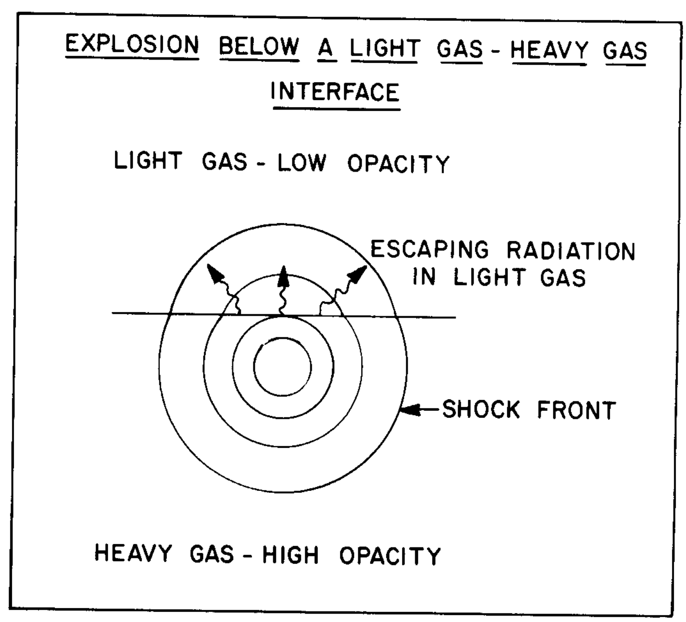

Fig. 4